In vitro Verification of a 3-D Regenerative Neural Interface Design: Examination of Neurite Growth and Electrical Properties Within a Bifurcating Microchannel Structure

Implantable devices that guide growth of multiple neurites are used to prompt cell separation and improve selective neural interfaces.

By P. A. Wieringa, R. W. F. Wiertz, E. L. de Weerd, and W. L. C. Rutten

ABSTRACT | Toward the development of neuroprosthesis, we propose a 3-D regenerative neural interface design for connecting with the peripheral nervous system. This approach relies on bifurcating microstructures to achieve defasciculated ingrowth patterns and, consequently, high selectivity. *In vitro* studies were performed to validate this design by showing that fasciculation during nerve regeneration can be influenced by providing a scaffold to guide growth appropriately. With this approach, neurites can be separated from one another and guided toward specific electrode sites to create a highly selective interface. The neurite separation characteristics were examined for smaller microchannel structures (2.5 and 5 μm wide) and larger microchannels (10 and 20 μm wide), with smaller microchannels shown to be statistically more effective at initiating separation. Electrodes incorporated at different locations within the microchannels allowed for the recording and tracking of action potential propagation. Microchannel size was also found to play an important role in this regard, with smaller microchannels amplifying the recordable extracellular

signal; a twofold increase in the signal to noise ratio was found for 5 μm wide microchannels.

KEYWORDS | Biomedical engineering; cellular engineering; guidance scaffold; neurite guiding; peripheral neuroprosthesis; regenerative neural interface; selectivity; tissue engineering

I. INTRODUCTION

A key challenge for neuroprosthetic advancement is the development of more effective neural interfaces. Issues for current interfacing strategies that must still be addressed include long-term biocompatibility and mechanical stability, ensuring an interface device is chronically implantable. The ability to maintain a stable association with a population of neurons, establish reliable recording and stimulation of this population, and, furthermore, to be able to do so with relatively high selectivity would provide a direct benefit to current neuroprosthetic technologies.

The ability to achieve a reliable association between electrodes and neurons is complicated by the fasciculated organization of neurons. Within the peripheral nervous system, neurons are bound together into fascicles and are very closely associated with one another. During natural development or regeneration of peripheral nerves, pioneering neurites use existing axons as a guiding scaffold which leads to this bundled, or fasciculated, composition [1].
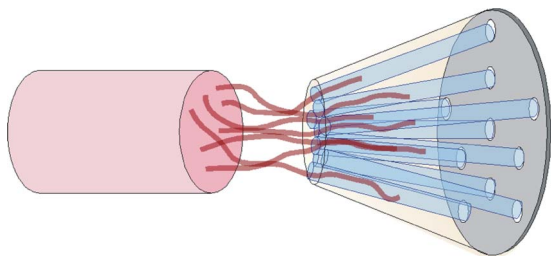
Fig. 1. *A rendition of the proposed 3-D regenerative neural interface, shown with regenerating neurites emanating from an abutted severed peripheral nerve and growing into the device. Visible are bifurcating, diverging microchannels intended to promote separation of neurites, subsequently guiding them toward individual electrode sites.*

This close proximity to one another presents a challenge when attempting to record from select neurons or set of neurons.

Current invasive techniques, such as the LIFE electrode or the Utah array, enable clear recordings from within the fascicle and permit a relatively high degree of selectivity [2], [3]. However, motion of the implant with respect to the surrounding neural tissue hinders chronic performance. Reliable contact can be compromised because of shifting position of the electrodes with respect to associated neurons. As well, this motion can result in an immune response, whereby subsequent damage to the surrounding tissue triggers encapsulation of the electrode by fibrous tissue [4]. The electrode becomes insulated from the surrounding neurons, hindering performance. To address these issues of creating a highly selective interface that is able to establish stable and reliable contact with a particular set of neurons, a three-dimensional regenerative neural interface is proposed (Fig. 1).

This approach is suitable for the severed peripheral nerves of amputees; the proximal end of a severed nerve is free to grow into the 3-D guidance scaffold of the interface and the fate of the distal nerve portion is of little concern. The general concept is to permit regrowing neurons to enter the 3-D scaffold, where they can be induced to separate from one another by virtue of the bifurcating scaffold design. The scaffold can then guide individual neurons toward incorporated electrode sites, allowing for a high degree of selectivity.

In addition to increased selectivity, it is possible that this approach will create neuroelectric contact that is more robust and reliable. Similar to the sieve electrode, mechanical stability should be inherent since the body effectively incorporates the interface into the neural tissue via the regenerating neurons [5]. As well, electrophysiological signal recording can be greatly improved when detecting signals within the confined spaces of the guidance scaffold [6]–[8]. This could greatly contribute to creating a more robust interface capable of very reliable recordings.

This study looks to validate *in vitro* the use of a 3-D bifurcating microchannel to initiate separated growth of regenerating neurons, countering fasciculation and making increased selectivity achievable. This builds on *in vitro* studies that have described neurite growth into enclosed microchannels, as well as on previous reports on the recording of neuroelectric activity from within microchannels [7]–[11]. Microchannels ranging from 2.5 to 20 μm wide are examined to see if this has an influence on the ability to counter fasciculation and to see if supporting evidence can be found for hypothesized mechanisms of initiating separated growth. The first hypothesis is that separation begins as a result of random growth cone exploration. With respect to microchannel design, a channel size that encourages these random deviations to encounter and interact with the bifurcating structure would better promote neurites to separate. The alternate proposed mechanism is volume limitation within the microchannel caused by preceding neurite growth, encouraging later neurites to grow down an alternate path with more available room.

Furthermore, an examination of recorded neural electrical activity within the microchannel is performed to further validate the proposed paradigm as a viable means of neural interfacing. The influence of microchannel size on electrical recording is also explored.

II. METHODS

A. Device Fabrication

To investigate neurite growth in bifurcating microchannels, a microfluidic device was created by reversibly sealing a polydimethylsiloxane (PDMS, Sylgard) overlay on to a suitable substrate that could serve as the culturing surface. To promote neuronal cell adhesion the substrate was treated for 2 hours with a 50 μg/ml solution of polyethyleneimine (PEI, Sigma Aldrich) [12]. The surface was then allowed to dry for 24 hours in a sterile flowhood.

The overlaying PDMS cast was created via micromolding with a silicon wafer mold, used to define two culturing chambers and a series of bifurcating microchannels connecting the two chambers. The wafer mold was created using a combination of SU8 structures, to define the open culturing chambers, and reactive ion etching (RIE) of the silicon wafer to form the microchannels (see Fig. 2) [13]. The resulting PDMS cast was dry-sterilized for 4 hours at 160 °C and then reversibly sealed, microchannels facing down, onto dry glass slips. The final culturing device pictured in Fig. 1 has an open "Origin" chamber and "Target" chamber connected via enclosed bifurcating microchannel networks.

The microchannels had a rectangular cross section with a single "Primary" channel bifurcating into two "Secondary" channels (Fig. 3). Channel height was 5 μm to prevent the migration of the whole cell body into the
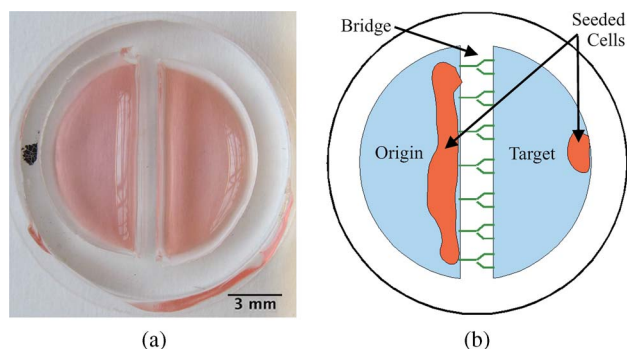
(a)   (b)

Fig. 2. *(a) Photograph of the device (scale bar 3 mm). (b) Depiction for clarification. The culturing device with the Origin chamber seeded with cells and the Target chamber with "Target" cells. The device has a 22 mm outer diameter, a 16 mm inner diameter and a Bridge width/channel length of 1 mm. PDMS cast height is 4 mm, resulting in 400 μL per chamber for culture medium. Channels are 2.5, 5, 10, and 20 μm wide, with 20 channels of each size.*

Fig. 4. *A modified microchannel for MEA layout, with electrodes positioned 200 μm apart to cover the channel length of 1 mm. Shown with electrode labels used during the study.*

microchannel [14]. Channel widths of 2.5, 5, 10, and 20 μm were optically examined, with each device having 20 channels of each size. Primary and Secondary channels both have identical cross sectional dimensions, with no dimensional changes after the bifurcation.

In preparation for cell culturing, the devices were first filled with a 70% ethanol solution. This ensured sterilization and permitted prefilling of the microchannels; the low surface tension of the ethanol solution allows fluid to completely fill the microfluidic channels, thus preventing trapped air bubbles within the microchannel networks. The ethanol solution was immediately followed by a double wash of MilliQ water (10 min per wash) and finally with a solution of sterile phosphate buffered solution (PBS) for approximately 2 hours.

For cell growth observations, a 26 mm diameter glass cover slip was used as a culturing surface suitable for optical examination. The parallel study of neurite electrical activity from within microchannels substituted the glass cover slip with a "200/30-i.R.-Ti- w/o" multielectrode array (MEA) from MultiChannel Systems (MCS)
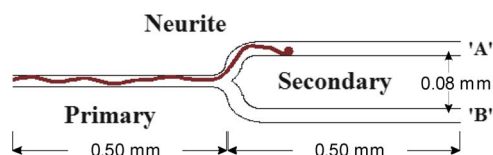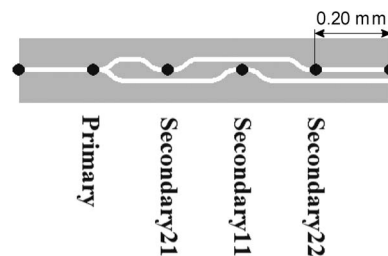
GmbH, Germany. The MEAs consist of a planar glass substrate incorporating 60 electrodes, 30 μm in diameter and 200 μm apart in an 8 × 8 grid, with leads insulated by an optically clear silicon dioxide layer.

The microchannels were redesigned to accommodate the MEA electrodes and the PDMS cast was carefully aligned on top of the electrode array with one electrode interfacing with one microchannel segment (Fig. 4), making possible electrical measurement of neurites within the microchannels as well as interfacing with cells in the two chambers. Electrodes within the microchannels were partially obscured by the PDMS cast, leaving an active electrode area having a width of the microchannel and approximately 30 μm in length.

B. Culture Preparation

To visually examine the separation properties of fasciculating neurites within bifurcating microchannels, cortical primary cells were selected over motor neurons or neurons from dorsal root ganglions (DRGs). Ease of acquisition of this cell type ensured a sufficient number of cells and high purity with respect to Glial cell content. In combination with serum-free R12 medium to reduce the rate of mitosis, a low number of Glial cells were maintained in cultures [15]. This allowed for observation of neuronal growth without interference from Glial cell growth.

The dissociated cortical neurons used were taken from 1–3 day old postnatal Wistar rats. The experiments were approved by the Animal Use Committee (DEC) of Leiden University and procedures were according to national and European guidelines. Briefly, rats were decapitated and cortices were dissociated from surrounding tissue. The cortical tissue pieces were placed in a tube of 3 ml of R12 culture medium. 1 ml of trypsin was added, incubated for 45 minutes at 37 °C, and the supernatant was removed and replaced by 0.5 ml of soybean trypsin inhibitor, 100 μL of DNAse, and enough R12 to obtain a total volume of 1 ml. The tissue was mechanically dissociated and the supernatant, containing the successfully dissociated cells, was removed and centrifuged at 1200 rpm for 5 minutes.

Fig. 3. *The bifurcating microchannel design with a pioneering neurite growing down the Primary channel and selecting a Secondary channel thereafter referred to as Secondary channel "A." The alternate vacant Secondary channel is designated "B." Both Primary and Secondary channels have the same widths. Channels with widths of 2.5, 5, 10, and 20 μm were investigated.*

The resulting pellet of dissociated cells was resuspended in a fresh volume of R12 medium to achieve a relatively high cell concentration (approx. 10×10^6 cells/mL).

To ensure the cell seeding was able to achieve a highly localized cell population, the PBS solution within the culturing chambers was removed and culture surfaces were permitted to dry for approximately 5 to 10 minutes; this ensured that the seeded cell concentration would not dilute in PBS and would remain localized within the seeding drop of R12. To prevent air bubbles from forming within the microchannels, thus blocking neurite growth, 30 μL of cell suspension was placed along the edge of the dividing bridge on the Origin chamber side *before* the PBS evaporated from within the microchannels. This created a highly localized monolayer of approximately 10 000 cells/mm^2. A small 15 μL drop was placed in the Target chamber at the point farthest from the microchannels to act as a distant target tissue (Fig. 2). The devices were placed for approximately 2 hours in an incubator maintaining 37 °C at 5% CO_2, allowing the neuronal cells to adhere to the glass slip surface. Each culture chamber was then filled with 400 μL of R12 and returned to the incubator, with medium refreshed every 3 days.

C. Growth Examination

After 2 days *in vitro* (DIV), the cultures were labeled using a 25 μM concentration of CellTracker Green (CTG) from Invitrogen in a solution of 25% DMSO and 75% DMEM. Medium was removed from each device chamber until only 50 μL remained per chamber, followed by the slow addition of 50 μL of CTG solution to create a final CTG concentration of 12.5 μM in each chamber. The devices were returned to the incubator for 45 minutes. Each chamber was then washed twice with DMEM and finally replaced with R12 medium. The cultures were returned to the incubator for 2 hours for optimal incubation of the fluorescent labeling agent before examination commenced.

Optical recording of neurite growth was performed using a Carl Zeiss Confocal Laser Scanning Microscope 510 with setting for FITC labeling. For long-term cell growth observation, the microscope was fitted with an environmental chamber to maintain cultures at a temperature between 35 and 37 °C and a gas concentration of 5% CO_2. An automated stage was constructed for time series image recording of neuronal growth at multiple locations within the culturing device. Cultures were observed 2 days after initial cell seeding over three days at $10\times$ magnification, with 15 minutes between concurrent images. Growth was recorded from 2.5, 5, 10, and 20 μm wide microchannels, with 20 of each size per device. Two devices from two separate platings were selected for evaluation.

The images were converted to videos using ImageJ [16], with automated image alignment performed using the TrakEm2 ImageJ plugin [17] to compensate for misalignment of the automated microscope stage. Neurite growth in the resulting videos was manually tracked using the MTrackJ ImageJ plugin [18] to ease identification and quantification of neural growth. Final video compression was performed using VirtualDub [19].

D. Growth Analysis

The neurite growth pattern within the microchannels was quantified, including only those microchannels in which growth was clearly observable past the bifurcation point. The quantification method assumed neurites proceeding through the microchannels in series, with the pioneering first neurite approaching the bifurcation and choosing a secondary path (at which point the chosen path was designated "A"; see Fig. 3). According to the mechanisms of fasciculation, later growing neurites are directed down Secondary path A because the preceding neurites are used as a guidance scaffold. A separation event is defined as the moment when at least one of the following neurites chooses the alternate secondary path "B."

To uncover possible neurite separation mechanisms, the number of neurites growing down Channel A *before* the separation event was noted (referred to as "prior-separation growth"). As well, growth observed in channels not experiencing a separation event (nonseparated growth) was recorded, with only nonseparation microchannels having more than one neurite included as only these could possibly experience separation. The average values and standard deviations were calculated for both cases. A measure of relative occupied volume was calculated by normalizing the average number of neurites by the channel width. The two hypotheses of random growth and volume limitation as mechanisms of separated growth were then assessed.

To validate the volume limitation mechanism, the occupied volume of prior-separation growth was compared to that of microchannels experiencing nonseparated growth (for microchannels of the same width) to see if a notable difference existed between the two different scenarios.

The prior-separation growth of different microchannel sizes was compared to test the random exploration hypothesis. Comparatively fewer fasciculating neurites before a separation event (less prior-separation growth) was interpreted as an increased ability to capitalize on growth cone deviations and initiate separation.

E. Electrical Examination

Electrical recording and stimulation used the MCS 1060BC preamplifier and an NI6071E acquisition card (National Instruments), sampling at 16 kHz, in conjunction with associated MCS software and a customized Labview application. A 2 week-old culture was examined with 2 microchannels of each width: 2.5, 5, 10 and 20 μm. Action potential (AP) recording used a detection threshold previously established to eliminate false positive detection in an open culture (no PDMS microchannels). This threshold is calculated as 5.5 times the estimated RMS noise value. Noise estimation was taken as the weighted average of the previous noise estimation and the RMS

calculated over the current 10 ms window. Since the experimental setup reduced electrode area by PDMS placement, thus theoretically translating to increased thermal noise, the measurement setup was first validated by examining the signal-to-noise ratio (SNR) to ensure neurite AP recording was still possible.

Point process analysis was employed to track individual AP propagation by virtue of the multiple electrode sites within the bifurcating microchannel. To isolate individual AP events, additional detection criteria eliminated compound APs resulting from the multiple neurites growing within a microchannel. After the Primary electrode (Fig. 4) detected an AP, a trailing 20 ms window was employed to find APs occurring at all electrode sites within the microchannel. The occurrence of these APs was accumulated into a latency histogram with a bin size of 0.0625 ms. For every AP detected at the Primary electrode, subsequent AP latency times were accumulated into a final histogram.

An examination of AP amplitude was also performed, looking at the effect of microchannel size on the recordable electrophysiological signal. To completely assess the ability to detect signals within the confined space of microchannels, these amplitudes were compared with the average recorded signal noise experienced at each electrode site.

III. RESULTS

A. Video Examination

The video analysis allowed for effective evaluation of ingrowing fasciculated neurite bundles within the bifurcating microchannel structure, provided neurites managed to grow into the microchannels. Video data were collected from two devices corresponding to two separate cell culture platings, respectively.

To investigate mechanisms of the observed neurite separation, the prior-separation growth was examined as well as the growth of microchannels experiencing no separation (nonseparated growth). Table 1 below shows the average number of neurites occupying channel A before the initial separation event occurs. Also shown is the average number of neurites recorded in channels experiencing no separation. To compare the influence of volume limitation on the induction of neurite separation, the relative occupied microchannel volume of both prior-separation and nonseparation growth is given as the average number of neurites normalized by microchannel width.

The comparison of occupied channel volume between channels experiencing separation and channels not experiencing separation show that nonseparated microchannels have, on average, more occupied volume then a microchannels with separated growth.

An initial one-way ANOVA analysis shows no statistically significant difference in average number of neurites between microchannel sizes. The normalized values of neurite growth also show no significant difference. To compensate for the small sample size of the 2.5 and 5 μm wide microchannels, these two categories are unified into a single "small channel" subgroup. Repeating the ANOVA analysis and performing additional posthoc Student T tests (two-tailed, 5% significance), it is revealed that the combined subgroup experienced less preseparation growth when compared to the two larger channel sizes.

Table 1 The Average Number of Ingrowing Neurites Before Separation Occurs (Prior-Separation Growth) Is Given in the Top Section of the Table, Followed by Neurite Growth Data for Microchannels Not Experiencing Separation (Nonseparation). The Final Section of the Table Shows the Average Neurite Growth Normalized by Microchannel Width, Providing a Comparison of Occupied Channel Volume Between Prior-Separation and Nonseparated Growth

Microchannel Size (µm)	2.5	5	10	20
Prior-separation Growth				
# of Microchannels	2	6	18	18
Total # of prior-separation neurites	3	6	50	74
Average # of prior-separation neurites	1.5	1	2.8	4.1
Standard Deviation	0.71	0	1.93	3.31
Non-separation Growth				
# of Microchannels	0	3	4	6
Total # of non-separation neurites	n/a	6	22	43
Average # of non-separation neurites	n/a	2	5.5	7.2
Standard Deviation	n/a	0	1.7	5.4
Growth Normalized by Channel Width				
Normalized Average # of prior-separation neurites (neurites/µm)	0.60	0.20	0.28	0.21
Normalized Average # of non-separation neurites (neurites/µm)	n/a	0.40	0.55	0.36

B. Electrical Examination

The electrical measurements were performed on a highly active cortical culture and the recorded activity was the result of spontaneous network bursts (i.e., synchronized electrical activity that is spontaneously intitiated in a region of the neuronal culture and spreads to the rest of the culture via synaptic connections). Of the eight possible bifurcating microchannels, two microchannels (one 20 and one 2.5 μm wide) exhibited poor activity; this was attributed to a slight misalignment of the PDMS overlay. The remaining 6 microchannels displayed notable electrical activity in both the Primary and Secondary channel branches. Approximately 323 500, 418 900, 402 200, and 89 800 APs were successfully detected from within the 2.5-, 5-, 10-, and 20-μm-wide microchannels, respectively, over a 12-hour period. An example of a detected AP is given in Fig. 5.

Successful tracking of action potentials within the microchannel network was performed, as shown in Fig. 6. The distinct histogram peaks of the point process analysis indicate that these action potential (AP) events are highly repeatable. This implies the same AP is being recorded later in time as it propagates down the microchannel. Note also that the histogram of the Primary electrode clearly shows a distinct period of no AP detection for approximately 1 ms following the initial AP detection (at time $=0$), corresponding well to the known refractory period of axons after experiencing an AP event.

In addition, since axons may have different diameters and, thus, different AP propagation velocities, differentiation between different-sized neurites based on their respective AP velocities should be possible. Fig. 6 shows two distinguishable peaks measured in the same channel and these peaks become further separated at an
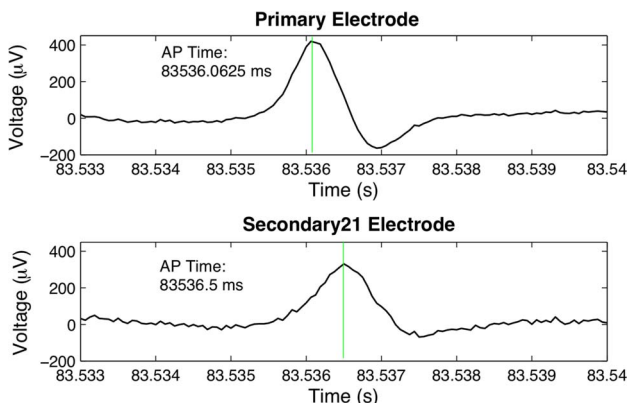

Fig. 6. *Point process analysis of AP propagation through the microchannel, represented as a histogram of # of recorded APs with respect to latency time of AP occurrence. Refer to Fig. 2(b) for designated electrode placement within the microchannel. For this example, 13 800 APs were detected at the Primary electrode. Fewer detections occurred at the Secondary 21 and Secondary 22 electrodes, with 556 and 2061 APs respectively. Note the peaks of recurring AP events(arrows).*

electrode further down the channel, indicating further velocity differentiation. The first peaks detected at the Secondary 21 and Secondary 22 electrodes correspond to velocities of 1.10 m/s and 0.37 m/s, respectively. If it assumed these values represent the propagation of the same AP, this implies that the conduction velocity decreases by a factor of 3 as the AP travels farther from the cell body. A similar reduction (factor of 2) is observed for the second distinct peak observed at Secondary 21 and Secondary 22 electrodes, with respective velocities of 0.32 m/s and 0.16 m/s.

The amplitude distribution of recorded APs per channel size, shown in Fig. 7 represented as the 5th to 95th percentile, is sufficiently above the mean detection threshold. Curve fitting of the detection threshold with respect to channel size (thus reduced electrode area) shows an inversely linear relationship. Based on the work presented in [6], a log-log curve was fit to the median AP amplitude. The 2.5-μm-wide channels exhibit signal amplification much lower than the expected log-log curve and, therefore, were excluded from the curve fitting.

IV. DISCUSSION

A. Initiation of Neurite Separation

To determine underlying mechanisms regarding the ability of a bifurcating microstructure to initiate neurite separation, the neurite growth pattern prior to the first separation event was examined to see if the combination of

Fig. 5. *An example of an action potential recorded from within a 5-μm-wide microchannel as it propagates from the Primary electrode to the Secondary21 electrode (see Fig. 4 for electrode locations). The latency of 0.4375 ms is calculated between the detected AP peaks (detection indicated by the green vertical line), translating to a conduction velocity of 0.457 m/s.*
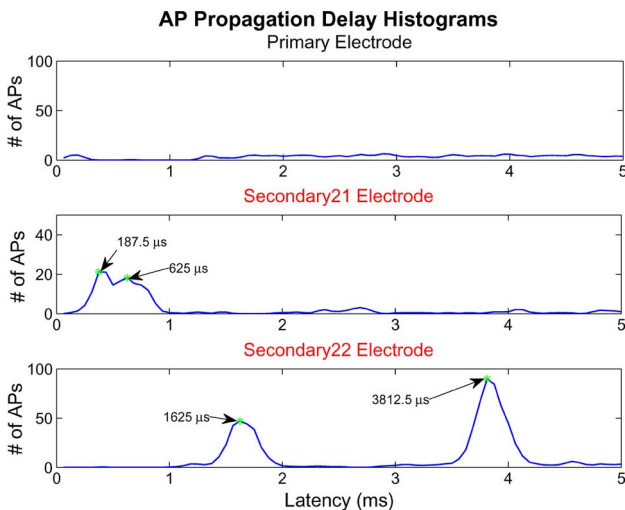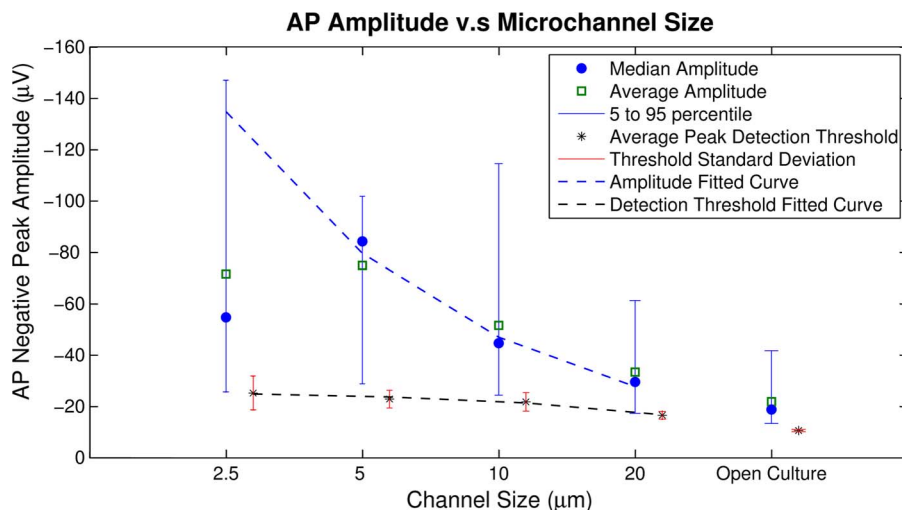
Fig. 7. *A comparison of AP amplitudes and AP detection levels for different microchannel sizes. Amplitude data includes the mean, median and errorbars showing the 5th to 95th percentile amplitude range. The detection level is represented by the mean value and the standard deviation. Based on modeling work by [6], the log-log equation* $\log(Amplitude) = -0.756 * \log(XArea) + 2.966$ *is fitted to the median amplitude data with an* $R^2 = 0.985$*; the 2.5 μm microchannel value is considered an outlier and is omitted. Amplitude refers to AP amplitude, XArea refers to the microchannel cross-sectional area (channel height of 5 μm). The mean detection threshold fitted curve, found to be* $Noise = -0.464 * ChannelWidth + 25.969$*, has an* $R^2 = 0.9761$*. Microchannel widths examined are 2.5, 5, 10, and 20 μm as well as electrodes located in "Open Culture."*

growth prior-separation and channel size somehow contributed to inducing neurites to separate. This analysis is performed within the context of two proposed mechanisms for the initiation of separation.

The first mechanism is volume limitation, whereby the secondary A channel becomes too full to support continued growth. This would prompt neurites to separate from the main bundle and select an alternate path with more available room. If this mechanism is indeed active, then channels that experience separation should have more ingrowth in secondary A channels at the moment before separation compared to channels exhibiting no separation at all. Otherwise, fasciculation is still dominant regardless of volume limitations and another reason must exist for the initial separation event.

Table 1 shows consistently more growth in nonseparated microchannels compared to equivalent prior-separation growth, invalidating the volume limitation hypothesis. Were this mechanism active, nonseparated channels would not consistently support more growth in channel A than the level of prior-separation growth observed in microchannels that experienced separation.

The alternate random growth hypothesis is based on the meandering exploratory growth behaviour of regenerating neurons. Growth cones were observed to deviate from the preceding neurite bundle, though they would generally return to the bundle mass. However, if the random exploration occurred near the bifurcation, this neurite would become segregated in the alternate secondary channel B. In this case, separated growth initiation can

be attributed to the random exploration of a neurite growth cone and the ability of the microchannel to "capture" these random deviations. Assuming growth deviations are of similar magnitudes in similar extracellular environments, this hypothesis implies that a microchannel design that better corrals growth into the vicinity of the bifurcation should improve the chances of a deviation being captured. Within the context of this study, narrower microchannels should exhibit an improved ability to initiate separation since the intrinsic confinement increases the likelihood of interaction between random growth deviations and the bifurcating structure.

Initially, the ANOVA analysis of the data in Table 3 resulted in no statistically significant differences between microchannel sizes with regards to separation initiation. However, it was noted that the 2.5- and 5-μm-wide microchannels had relatively small sample sizes. To compensate, these two categories were combined to form a "small channel" subgroup. Reapplying the ANOVA analysis revealed that smaller channels are better able to initiate separation. Therefore the hypothesis of separation initiation by random growth cone exploration is supported. Microchannel designs that take advantage of this mechanism to "capture" such random events can be incorporated into final scaffold design strategies, promoting neurite separation toward the intended selective neural interface.

B. Electrical Recording Within a Guidance Scaffold

Analysis of the neuroelectric activity using the experimental setup described showed that action potentials

could be both clearly recorded within the confined microstructure as well as successfully tracked as an AP propagated past the multiple electrode sites within the PDMS guidance scaffold. As well, conduction velocities could be estimated, with reported values of 1.10 m/s to 0.16 m/s falling within the range of previously reported conduction velocities [8], [20].

Further observations suggest that, via this tracking of AP propagation, it is also possible to distinguish different neurites based on different propagation velocities. This has direct implications for neural interfacing applications; by employing two or more electrodes within a scaffold microchannel, one can differentiate signals even in the presence of fasciculated growth. This method is only practical in the chronic setting since neurite diameter, and thus AP conduction velocity, changes during maturation. A suggested artifact of this is the observed decrease in conduction velocity at different points further along the microchannel, thought to be the result of neurite diameter reduction along the length of the immature regenerating axon toward the growth cone. Once regeneration has been completed and ingrowth into the 3-D scaffold has stabilized, this strategy of multiple electrode sites could lead to a further increase in selective neural contact.

Additional evaluation of AP amplitude corroborates the theory of signal amplification of APs recorded within a microchannel. This result was predicted by Fitzgerald *et al.*, who suggested amplification would occur if the extracellular volume was sufficiently reduced relative to the neurite diameter [6]. Comparatively, the resulting slope of -0.756 from curve fitting the median amplitude values compares well with that estimated from [6] (-0.783).

It should also be noted that maximum amplification appears to be achieved for a microchannel size of 5 μm, indicating a possible optimal arrangement. Signals recorded within these microchannels exhibit a signal-to-noise ratio of approximately 3.6, higher than that observed for other microchannels and constituting a twofold increase compared to recordings in open cultures without PDMS scaffolding present. Especially striking is the apparent decrease in signal strength for the 2.5 μm wide channels. Although still adequately above the detection threshold, this is significantly lower than the expected amplitude. This indicates a possible change in the amplification mechanism as the microchannel passes a threshold size, suggesting a potential optimization is necessary that strikes a balance between signal/noise amplification and other additional factors, such as sufficient channel size to allow extracellular volume reduction while permitting neural maturation and subsequent larger extracellular ionic flows.

Both results support the proposed interfacing paradigm, with a potential to improve both selectivity as well as the strength of the recorded signals.

V. CONCLUSION

In general, this study has shown the validity of the proposed 3-D guidance scaffold as part of a neural interfacing strategy. Bifurcating microchannel structures are able to initiate the separation of an ingrowing bundle of neurites into smaller bundles, with the inference that the mechanism for this initiation is the effective capture of random growth cone explorations. A smaller microchannel structure better capitalizes on this by confining growth within the proximity of the bifurcation point, resulting in separated growth and leading to improved selective contact for the described application.

The electrical component of the study revealed that recording within such a 3-D guidance scaffold amplified AP signals and improved the signal-to-noise ratio, with evidence of an optimal microchannel size for reasons yet to be determined. Furthermore, the ability to measure from multiple locations along the same bundle of ingrowing neurites within the scaffold allowed for specific neurons to be distinguished based on differences in AP conduction velocities. This strategy could also be implemented in a neural interface as a means of further improving selectivity despite the occurrence of fasciculated growth. ∎

REFERENCES

[1] C. Ide, "Peripheral nerve regeneration," *Neurosci. Res.*, vol. 25, no. 2, pp. 101–121, Jun. 1996.

[2] X. Navarro, T. B. Krueger, N. Lago, S. Micera, T. Stieglitz, and P. Dario, "A critical review of interfaces with the peripheral nervous system for the control of neuroprostheses and hybrid bionic systems," *J. Peripheral Nervous Syst.*, vol. 10, pp. 229–258, 2005.

[3] W. L. C. Rutten, "Selective electrical interfaces with the nervous system.," *Annu. Rev. Biomed. Eng.*, vol. 4, pp. 407–452, 2002.

[4] D. J. Edell, V. Van Toi, V. M. McNeil, and L. D. Clark, "Factors influencing the biocompatibility of insertable silicon microshafts," *IEEE Trans. Biomed. Eng.*, vol. 39, no. 6, pp. 635–643, Jun. 1992.

[5] N. Lago, E. Udina, A. Ramachandran, and X. Navarro, "Neurobiological assessment of regenerative electrodes for bidirectional interfacing injured peripheral nerves," *IEEE Trans. Biomed. Eng.*, vol. 54, no. 6, pp. 1129–1137, Jun. 2007.

[6] J. J. Fitzgerald, S. P. Lacour, S. B. McMahon, and J. W. Fawcett, "Microchannels as axonal amplifiers," *IEEE Trans. Biomed. Eng.*, vol. 55, no. 3, pp. 1136–1146, Mar. 2008.

[7] R. Morales, M. Riss, L. Wang, R. Gavín, J. A. Del Río, R. Alcubilla, and E. Claverol-Tinturé, "Integrating multi-unit electrophysiology and plastic culture dishes for network neuroscience.," *Lab on a Chip*, vol. 8, pp. 1896–1905, 2008.

[8] B. J. Dworak and B. C. Wheeler, "Novel MEA platform with PDMS microtunnels enables the detection of action potential propagation from isolated axons in culture," *Lab on a Chip*, vol. 9, p. 404, 2009.

[9] J. W. Park, B. Vahidi, A. M. Taylor, S. W. Rhee, and N. L. Jeon, "Microfluidic culture platform for neuroscience research," *Nat. Protocols*, vol. 1, pp. 2128–2136, Dec. 2006.

[10] E. Claverol-Tinturé, J. Cabestany, and X. Rosell, "Multisite recording of extracellular potentials produced by microchannel-confined neurons in-vitro," *IEEE Trans. Biomed. Eng.*, vol. 54, no. 2, pp. 331–335, Feb. 2007.

[11] F. Morin, N. Nishimura, L. Griscom, B. Lepioufle, H. Fujita, Y. Takamura, and E. Tamiya, "Constraining the connectivity of neuronal networks cultured on microelectrode arrays with microfluidic techniques: A step towards neuron-based

functional chips," *Biosens. Bioelectron.*, vol. 21, pp. 1093–1100, 2006.

[12] A. R. Vancha, S. Govindaraju, K. V. L. Parsa, M. Jasti, M. González-García, and R. P. Ballestero, "Use of polyethyleneimine polymer in cell culture as attachment factor and lipofection enhancer," *BMC Biotechnol.*, vol. 4, p. 23, Oct. 2004.

[13] J. C. McDonald, D. C. Duffy, J. R. Anderson, D. T. Chiu, H. Wu, O. J. Schueller, and G. M. Whitesides, "Fabrication of microfluidic systems in poly(dimethylsiloxane)," *ElectrophoResis*, vol. 21, no. 1, pp. 27–40, Jan. 2000.

[14] M. P. Maher, J. Pine, J. Wright, and Y. C. Tai, "The neurochip: A new multielectrode device for stimulating and recording from cultured neurons," *J Neurosci. Methods*, vol. 87, no. 1, pp. 45–56, Feb. 1999.

[15] H. J. Romijn, F. Van Huizen, and P. S. Wolters, "Towards an improved serum-free, chemically defined medium for long-term culturing of cerebral cortex tissue," *Neurosci. Biobehav. Rev.*, vol. 8, no. 3, pp. 301–334, 1984.

[16] W. S. Rasband. (2009). *ImageJ*, NIH, Bethesda, MD. [Online]. Available: http://rsb.info.nih.gov/ij/

[17] A. Cardona and R. Douglas. (2008). *TrakEm2*, Institute of Neuroinformatics, Zurich. [Online]. Available: http://www.ini.uzh.ch/~acardona/trakem2.html

[18] E. Meijerink. (2008). *MTrackJ*, Erasmus MC, Rotterdam. [Online]. Available: http://www.imagescience.org/meijering/software/

[19] A. Lee. (2008). *VirtualDub*. [Online]. Available: http://www.virtualdub.org/

[20] J. B. Colombe and P. S. Ulinski, "Temporal dispersion windows in cortical neurons," *J. Comput. Neurosci.*, vol. 7, pp. 71–87, 1999.

ABOUT THE AUTHORS

Paul Andrew Wieringa was born in Owen Sound, ON, Canada, in 1980. He received the B.A.Sc. degree from the University of British Columbia (UBC), Vancouver, Canada, in 2004 and the M.Sc. degree in electrical engineering from the University of Twente (UT), Enschede, the Netherlands, in 2008. He is currently working toward the Ph.D. degree at the Scuola Superiore Sant'Anna, Pisa, Italy.

He remained at UT as a Research Associate with the Biomedical Signals and Systems Group from 2008 to 2009. His main area of interest is the development of regenerative neural interfaces, focusing on aspects of neural tissue engineering and tissue scaffold micro/nanofabrication.

Remy W. F. Wiertz was born in Hengelo, the Netherlands, in 1974. In 2000 he received the B.S. degree in life science from the Saxion Hogeschool, Deventer, the Netherlands. He is currently working toward the Ph.D. degree in the Biomedical Signals and Systems Group, University of Twente (UT), Enschede, the Netherlands.

In 2001, he started working as a lab technician in the Biomedical Signals and Systems Group at UT. His main areas of interest are neural engineering and neuronal adhesion.

Eddy L. de Weerd studied electrical engineering and materials science at the University of Twente, Enschede, the Netherlands.

He is a researcher in microfluidics and nanofluidics in the BIOS/Lab on a Chip group (MESA+ Institute for Nanotechnology, University of Twente). After finishing his studies, he has worked in sensor research and development for several Dutch companies, mainly involved in technology transfer. His research interests include micro- and nanosensors and actuators, electrochemistry, and reliability of microsystems.

Wim L. C. Rutten was born in 1950. He received the Ph.D. degree in solid state physics from Leiden University, Leiden, the Netherlands, in 1979.

He was trained as an Experimental Physicist at Leiden University. He worked as Physicist-Audiologist with Leiden University Hospital in hearing science and electrophysiology until 1985, before joining the Biomedical Engineering Group at the University of Twente, Enschede, the Netherlands. He is currently Professor of Neural Engineering with the Faculty of Electrical Engineering, Mathematics and Computer Science and with the Institute for Biomedical Technology (MIRA) of the University of Twente. He is the Leader of the Neural and Cellular Engineering Program of MIRA, with a focus on live learning (cultured) neural networks, the development of a cultured probe-neural prosthesis, and on (EEG-based) brain–computer interfaces.